

## A role for *Pax-1* as a mediator of notochordal signals during the dorsoventral specification of vertebrae

Haruhiko Koseki<sup>1</sup>, Johan Wallin<sup>1</sup>, Jörg Wilting<sup>2</sup>, Yoko Mizutani<sup>1</sup>, Andreas Kispert<sup>3</sup>, Cecilia Ebensperger<sup>2</sup>, Bernhard G. Herrmann<sup>3</sup>, Bodo Christ<sup>2</sup> and Rudi Balling<sup>1,\*</sup>

<sup>1</sup>Department of Developmental Biology, Max-Planck-Institute of Immunobiology, Stübeweg 51, W-79108 Freiburg, Germany

<sup>2</sup>Department of Anatomy, Freiburg University, Albertstrasse 17, W-79104 Freiburg, Germany

<sup>3</sup>Department of Biochemistry, Max-Planck-Institute of Developmental Biology, Spemannstrasse 35, W-72076 Tübingen, Germany

\*Author for correspondence

### SUMMARY

The notochord plays an important role in the differentiation of the paraxial mesoderm and the neural tube. We have analyzed the role of the notochord in somite differentiation and subsequent formation of the vertebral column using a mouse mutant, *Danforth's short-tail* (*Sd*). In this mutant, the skeletal phenotype is most probably a result of degeneration and subsequent loss of the notochord. The *Sd* gene is known to interact with *undulated* (*un*), a sclerotome mutant. Double mutants between *Sd* and *un* alleles show an increase in the severity of the defects, mainly in the ventral parts of the vertebrae. We also show that part of the *Sd* phenotype is strikingly similar to that of the *un* alleles. As *un* is known to be caused by a mutation in the *Pax-1* gene, we analyzed *Pax-1* expression in *Sd* embryos. In *Sd* embryos, *Pax-1* expression is reduced, providing a potential molecular basis for the genetic interaction observed. A complete loss of *Pax-1* expression in mor-

phologically intact mesenchyme was found in the lower thoracic-lumbar region, which is phenotypically very similar to the corresponding region in a *Pax-1* null mutant, *Undulated short-tail*. The sclerotome developmental abnormalities in *Sd* coincide closely, both in time and space, with notochordal changes, as determined by whole-mount T antibody staining. These findings indicate that an intact notochord is necessary for normal *Pax-1* expression in sclerotome cells, which is in turn required for the formation of the ventral parts of the vertebrae. The observed correlation among structural changes of the notochord, *Pax-1* expression levels and skeletal phenotypes, suggests that *Pax-1* might be an intrinsic mediator of notochordal signals during the dorsoventral specification of vertebrae.

Key words: *Danforth's short-tail*, *undulated*, notochord, *Pax-1*, sclerotome differentiation, dorsoventral specification

### INTRODUCTION

The axial skeleton of vertebrates is composed of a metameric series of vertebral bodies and intervertebral discs. Both of these structures are derived from the sclerotome. Sclerotome cells are generated as a consequence of the differentiation of somites into the mesenchymal sclerotome and epithelial dermomyotome. After deepithelialization of somites, medial sclerotome cells migrate and proliferate towards the notochord to form the anlagen of vertebral bodies and intervertebral discs, whereas the lateral sclerotome cells form the pedicles and laminae of neural arches and ribs (Christ and Wilting, 1992).

The notochord has an important role in the dorsoventral specification of not only the neural tube (reviewed by Jessell et al., 1989; van Straaten and Heckking, 1991; Placzek et al., 1990; Yamada et al., 1991), but also the paraxial mesoderm (Watterson et al., 1954; Avery et al., 1956; Cooper, 1965; Youn and Malacinski, 1980). The influence

of the notochord on somite differentiation has been analyzed mainly in avian and amphibian embryos treated surgically or chemically to remove the notochord and/or the neural tube. These results suggest that the notochord is required for proper formation of the cartilaginous axial skeleton from somites.

The availability of mouse notochord mutants allows a genetic approach to analyze the function of the notochord in skeletal development. *Danforth's short-tail* (*Sd*) is a skeletal mutant in which the notochord is affected (Dunn et al., 1940). The gene responsible for the *Sd* mutation maps to the proximal part of mouse chromosome 2 and has not yet been identified. Grüneberg (1958) and Gluecksohn-Schoenheimer (1945) indicated that the abnormalities of the vertebral column in *Sd* embryos were a result of structural changes of the notochord, particularly, in the tail region of day 10.5 embryos. Histochemical changes of the notochord and the perichordal sheath were shown to occur earlier, suggesting that the primary abnormality is indeed in the

notochord (Paavola et al., 1980; Center et al., 1982). Therefore, the various morphological defects of the vertebrae are considered to reflect the absence of the notochord as a primary defect in *Sd*. Our interest in *Sd* is based on a genetic interaction between *Sd* and *undulated* (*un*). Crossing the two mutants resulted in an increase in the severity of the skeletal phenotype, particularly in the vertebral bodies of cervical vertebrae (Wright, 1947; Grüneberg, 1953). Since *un* is caused by a mutation in the *Pax-1* gene (Balling et al., 1988; Dietrich, Gruss and Balling, unpublished data), this suggests an underlying interaction between the notochord and *Pax-1*-expressing sclerotome cells.

*Pax-1* is a DNA-binding transcriptional activator identified as a result of its sequence similarity with *Drosophila* paired-box containing genes (Bopp et al., 1986; Deutsch et al., 1988; Chalepakis et al., 1991). *Pax-1* is expressed in the developing sclerotome, pharyngeal pouches, facial mesenchyme, limb buds and thymus during embryogenesis (Deutsch et al., 1988; Koseki and Balling, unpublished data). The *Pax-1* locus has been demonstrated to be altered in three *undulated* alleles; *undulated* (*un*), *undulated-extensive* (*un<sup>ex</sup>*) and *Undulated-short tail* (*Un<sup>s</sup>*) (Balling et al., 1988; Dietrich, Gruss and Balling, unpublished data). In all *un* alleles, the development of the vertebral column is affected, resulting in the lack or deformity of vertebral bodies and intervertebral discs (Balling et al., 1991). As the *un* mutation affects the differentiation of the sclerotome cells into the axial skeleton (Grüneberg, 1954), *Pax-1* seems to play a key role in this process.

The purpose of this study was to analyze the role of the notochord and *Pax-1* during differentiation of the sclerotome. To this end we analyzed the expression of *Pax-1* in *Sd* mutant embryos. We tried to correlate three aspects; the skeletal phenotype, *Pax-1* expression and histochemical changes of the notochord in *Sd*. Our studies provide evidence that *Pax-1* is required for the specification of the ventral parts of the vertebrae in response to notochordal signals.

## MATERIALS AND METHODS

### Animals

RSV mice carrying the *Danforth's short-tail* (*Sd*) mutation were obtained from the Jackson Laboratories. *Undulated-short tail* (*Un<sup>s</sup>*) and *undulated-extensive* (*un<sup>ex</sup>*) mutant mice were kindly provided by Dr A. M. Malashenko, Krosnogorsk, Russia and Dr J. L. Cruickshank, Leeds, England, respectively. These mutants were backcrossed onto C57BL/6 background. In the case of *Sd* mutants, N3 or N4 heterozygotes were used to obtain homozygous embryos. N1 to N4 mice were utilized in *Un<sup>s</sup>* and *un<sup>ex</sup>* mutants. Embryos were recovered on days 9-19 of gestation where day 0.5 is 12 a.m. on the day of detection of the vaginal plug. For the genotyping of *Sd* embryos, embryonic DNA was extracted from the yolk sac and subjected to a genotype analysis using the microsatellite PCR primers for the *D2Mit7* locus (Dietrich et al., 1992). *D2Mit7* is localized 6.2±1.7 cM distal from the *Sd* locus and is polymorphic between C57BL/6 and RSV (Koseki et al., 1993). Genotypes of *Un<sup>s</sup>* and *un<sup>ex</sup>* newborn mice were determined by DNA blot analysis using a *Pax-1* probe.

### Skeletal preparations

Skeletal preparations were made by an alcian blue-alizarin red

staining procedure, using the protocol described by Kessel et al. (1990). Photographs were taken under the stereomicroscope using a flashlight unit originally prepared for the duplication of slides. The number of vertebrae was scored starting with the atlas as the first vertebra.

### RNase protection assay

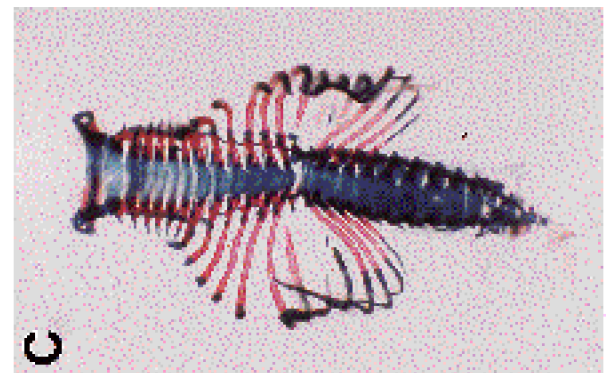
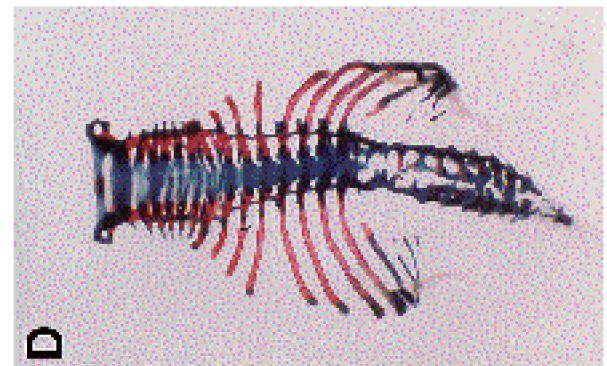
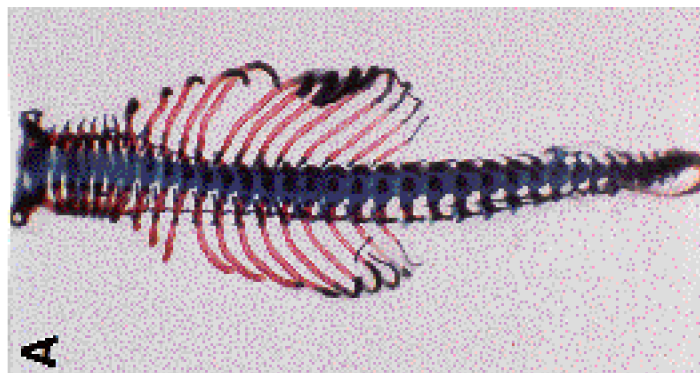
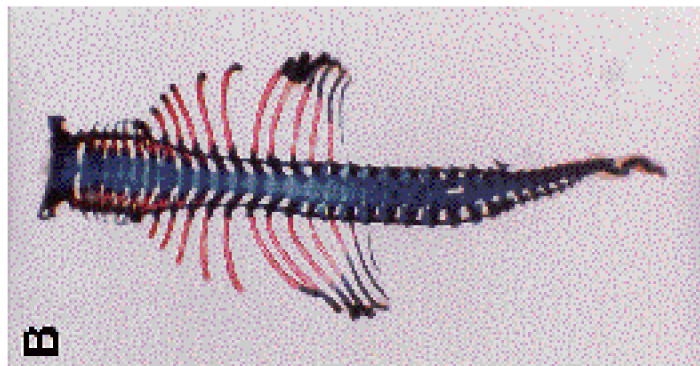
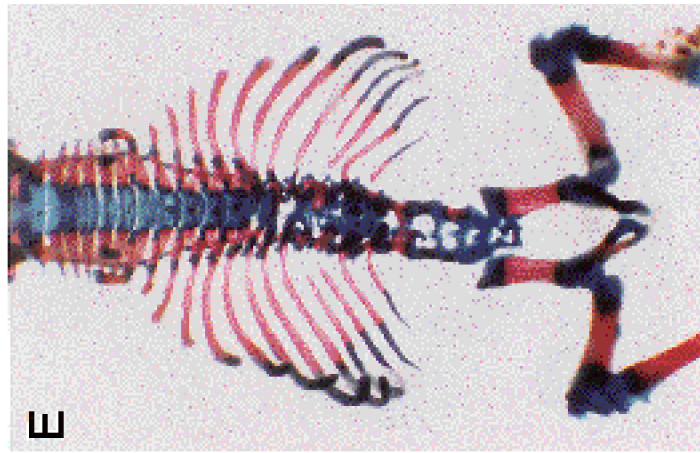
Total cellular RNA was isolated from day-10.5 p.c. and day-13.5 p.c. embryos by the guanidine/cesium chloride method (Glisin et al., 1974). RNase protection assays were performed as described (Melton et al., 1984). The *Pax-1 HincII-SacI* paired box fragment which was cloned into the *SmaI* site of pSPT18 (Deutsch et al., 1988) was linearized with *HindIII* and was transcribed with T7 RNA polymerase to generate a 377 nucleotide antisense riboprobe.  $\alpha$ -tubulin (*M $\beta$ 5*) was used as an internal control to quantify the amount of *Pax-1* transcripts (Wang et al., 1986). pBluescriptIIKS vector carrying the *BamHI-SacII* fragment was linearized with *HindIII* and subjected to subsequent in vitro transcription using T7 RNA polymerase to generate a 306 nucleotide riboprobe. Radioactivities of the protected RNA fragments were quantified using a Bio Image Analyzer (Fujix BAS2000, Fuji film).

### In situ hybridization

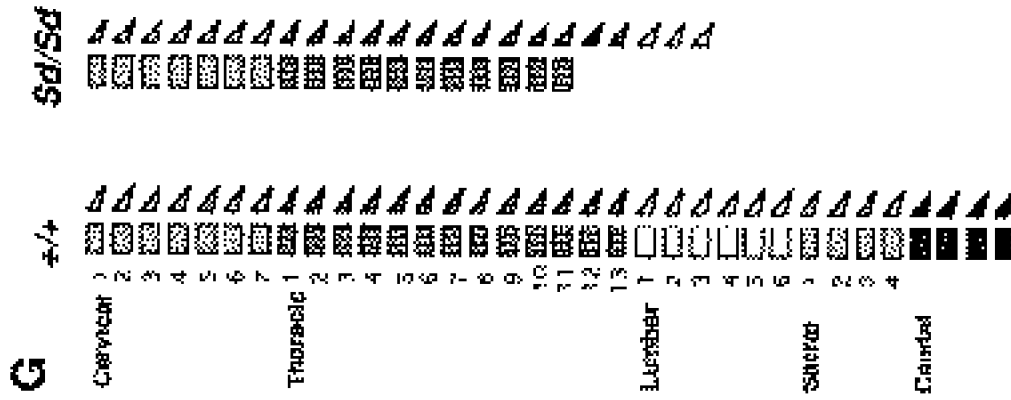
Embryos were fixed overnight in 4% paraformaldehyde in phosphate-buffered saline (PBS), and then embedded in paraffin wax. Sections were cut at 6  $\mu$ m and placed onto 3-aminopropyltriethoxysilane (TESPA)-coated slides. The sections were subjected to in situ hybridization as described (Kessel and Gruss, 1991). The *Pax-1* probe was transcribed from the same construct as used for RNase protection. For *Pax-3* hybridization, a *HindIII-PstI* 516 nucleotide fragment of the mouse *Pax-3* cDNA was used after alkaline hydrolysis (Goulding et al., 1991). *M-twist* expression was investigated with the riboprobe generated from a *XbaI-EcoRI* 425 nucleotide fragment (Wolf et al., 1992).

Whole-mount in situ hybridization was performed according to the protocol devised by Rosen and Beddington (1993) using digoxigenin-11-UTP labeled riboprobes. Embryos were cleared using a mixture of benzbenzoate and benzylalcohol (2:1) after

**Fig. 1.** Enhanced severity of skeletal phenotype as a consequence of a genetic interaction between *Sd* and *Un<sup>s</sup>*. Vertebral columns of day-17.5 fetuses with the following genotypes are shown; (A) +/+/+, (B) *Un<sup>s</sup>* +/+, (C) + *Sd*/+ and (D) *Un<sup>s</sup>* *Sd*/+. Specimens are stained with the alcian blue-alizarin red procedure. Skulls, distal parts of ribs, fore- and hind-limbs were removed. (A) Ossification centres are already formed in wild-type fetuses at this stage. (B) *Un<sup>s</sup>* single heterozygotes show a delay in the formation of ossification centres and occasional splits of vertebral bodies in the lumbosacral region. The 13th pair of ribs is floating. (C) *Sd* single heterozygotes also exert a delay in the ossification of vertebral bodies and occasional splits in the midline are observed as in *Un<sup>s</sup>* single heterozygotes. The number of vertebral bodies are 30 on average, ranging from 27 to 36. (D) Compound heterozygotes between *Un<sup>s</sup>* and *Sd* show stronger defects in the caudal half of the axial skeleton than either of the single heterozygotes. In regions posterior to the 8th thoracic vertebra, vertebral bodies and intervertebral discs are completely lost and pedicles of neural arches are protruding towards the midline without fusion. Lower ribs are also floating. (E) *Sd* homozygotes at newborn stage. (F) The number of vertebral bodies, neural arches and ribs was compared between *Sd* homozygotes and wild type. Standard deviations are indicated. The number of specimens examined in each genotype was also shown. (G) The skeletal phenotype of wild type and *Sd* homozygote is schematically illustrated. Note the persistence of neural arches in the thoracolumbar region of *Sd* homozygotes, where vertebral bodies are absent.



	<i>+/+</i> (n=10)	<i>Sd/Sd</i> (n=12)
Vertebral bodies	60±2.5	18±2.8
Neural arches	35±1.4	28±1.7
Ribs	13±0	12±1.3



**G**

equilibration with absolute methanol, and scored and photographed under the stereomicroscope.

### Whole-mount immunostaining

The antiserum against the T-protein was raised by immunization of rabbits with bacterially expressed protein and was affinity purified (Kispert and Herrmann, 1993). After fixation in 4% paraformaldehyde in PBS, embryos were soaked in absolute methanol, treated with 1 M Glycine (pH 7-8) and 3% H<sub>2</sub>O<sub>2</sub> in PBS, washed briefly with PBST (0.2% BSA and 0.1% Triton X-100 in PBS), incubated in PBSTN (0.2% BSA, 0.1% Triton X-100 and 5% fetal calf serum in PBS) and subjected to staining reaction with affinity-purified T antiserum diluted 1:500 to 1:1000 in PBSTN at 4°C overnight. After extensive washing with PBST, they were incubated with goat-anti-rabbit Ig conjugated with peroxidase diluted 1:400 in PBSTN for 2 hours at room temperature. Peroxidase coupled secondary antibody was detected by incubation with 0.3 mg/ml diaminobenzidine (DAB) and 0.03% H<sub>2</sub>O<sub>2</sub> in PBS. The reaction was stopped by washing with PBS twice. Embryos were cleared using a mixture of benzbenzoate and benzylalcohol (2:1) after equilibration with absolute methanol, and then scored and photographed under the stereomicroscope.

## RESULTS

### A genetic interaction between *Sd* and *Un<sup>s</sup>*

In the original studies (Wright, 1947; Grüneberg, 1953) the *un*-allele was used to show a genetic interaction between *Sd* and *un* whereas in the present study we used the *Un<sup>s</sup>*-allele to analyze the basis of this genetic interaction. *Un<sup>s</sup>* is a complete deletion of the *Pax-1* locus. The skeletal phenotype of day-17.5 fetuses from matings between *Un<sup>s</sup>* and *Sd* heterozygotes was investigated. Double heterozygous mice carrying both mutations (*Sd*/+, *Un<sup>s</sup>*/+) were much more severely affected than either of the single heterozygotes (Fig. 1A-D). Although in the single heterozygotes the vertebral bodies were only slightly affected in the thoracolumbar region, almost a complete loss of vertebral bodies was observed in the thoracolumbosacral region of the double mutants. The cervicothoracic region of these double heterozygotes was less affected than the more caudal part, but an interaction between the two genes was confirmed at all levels of the vertebral column by determination of the dorsoventral diameter of the vertebral bodies (data not shown). The length of the tail was shorter in the compound heterozygotes compared to single heterozygotes.

### *Pax-1* expression in *Sd* mutant embryos

In order to explain the molecular basis of this genetic interaction we analyzed whether the expression of *Pax-1* was changed in *Sd* embryos. First, the amount of *Pax-1* mRNA was compared to that of *Mβ5*, one of the  $\beta$ -tubulin gene isoforms, using RNase protection analysis (data not shown). The *Mβ5* gene is a component of the cytoskeleton, which is expressed in a ubiquitous manner (Wang et al., 1986). While no significant change was observed in *Sd* homozygotes at day 10.5, *Pax-1* expression was reduced to 40% of the wild-type level in day-13.5 p.c. *Sd* homozygotes. Compound heterozygotes between *Sd* and *Un<sup>s</sup>* express less *Pax-1* than either of the single heterozygotes (data not shown). Therefore, an interaction between the *Sd* and *Un<sup>s</sup>* mutation leads to a reduction in the level of *Pax-1* expression.

In order to determine whether *Pax-1* expression is affected in a tissue-specific or in a widespread manner, we carried out an in situ RNA hybridization analysis. Based on the results of the RNase protection analyses, *Pax-1* expression was first investigated in day-13.5 embryos (Fig. 2). In wild-type embryos *Pax-1* was expressed along the entire axis in the region surrounding the anlagen of the vertebral bodies, the pedicles of the neural arches and the proximal parts of the ribs. In addition, *Pax-1* expression was observed in the thymus, the mesenchyme of the lower jaw, the sternum and limb buds (data not shown). Parasagittal sections indicated the existence of more than 40 *Pax-1*-expressing segmental domains along the developing vertebral column. However, in the axial skeleton of *Sd* homozygotes, *Pax-1* expression stopped abruptly in the thoracic region (Fig. 2C). In three embryos analyzed, only 14, 17 and 18 *Pax-1*-expressing domains, respectively, were found. In *Sd* homozygotes no cartilaginous tissues were seen in the more caudal region, correlating with the absence of *Pax-1* expression (Fig. 2E,F).

The initial changes of *Pax-1* expression in *Sd* homozygotes were traced back to the period between day-9.5 to -10.5 p.c.. At day 9.5 (with 20-25 somites) only a few *Sd* homozygotes were affected (data not shown). However, at day 10.5 (with 35-40 somites) *Pax-1* expression in the posterior part of *Sd* homozygotes was affected without exception (Fig. 3). In wild-type embryos, *Pax-1* expression was observed along the entire body axis from the occipital bone anlage to the newly generated somites in the tail region (Fig. 3 and Koseki and Balling, unpublished observations). *Pax-1* expression was stronger in the caudal half and a small area in the most cranial part of each segmental unit (distinguished by bars in Fig. 3). In the cervical region of *Sd* homozygous and wild-type embryos, no differences in the expression of *Pax-1* could be seen (Fig. 3). *Pax-1* expression was seen up to the thoracic region of *Sd* homozygotes and could not be observed in the lumbar, sacral or caudal regions (Fig. 3). Other *Pax-1* expression domains, including the forelimb and hindlimb bud and pharyngeal pouches, were not affected (Fig. 3). In seven *Sd* homozygotes the number of *Pax-1*-expressing sclerotomes starting from the proatlas anlage was 17 on average. This is similar to what was observed in day-13.5 embryos.

### The *Sd* and *un* mutations both affect the ventral structures of vertebrae

As the expression of *Pax-1* is affected in both mutants, *Sd* and *un*, we were interested to analyze the phenotypic consequences of the loss or the reduction of *Pax-1* expression. A remarkable change in *Sd* homozygotes was the truncation of the axial skeleton (compare Fig. 1A and E). The severity of defects along the anterior-posterior (A-P) axis of the vertebral column increased in the thoracolumbar region. *Sd* homozygotes had, on average, 18 vertebral bodies (ranging from 14 to 20), 23 neural arches (ranging from 21 to 25) and 12 ribs (ranging from 10 to 13) indicating that the formation of the vertebral bodies stopped around the 11th thoracic vertebra, whereas neural arches were formed up to the 3rd lumbar vertebra (Fig. 1F). In the caudal part of the truncated axial skeleton of *Sd* homozygotes, ventral structures such as the vertebral bodies, the intervertebral discs and the pedicles

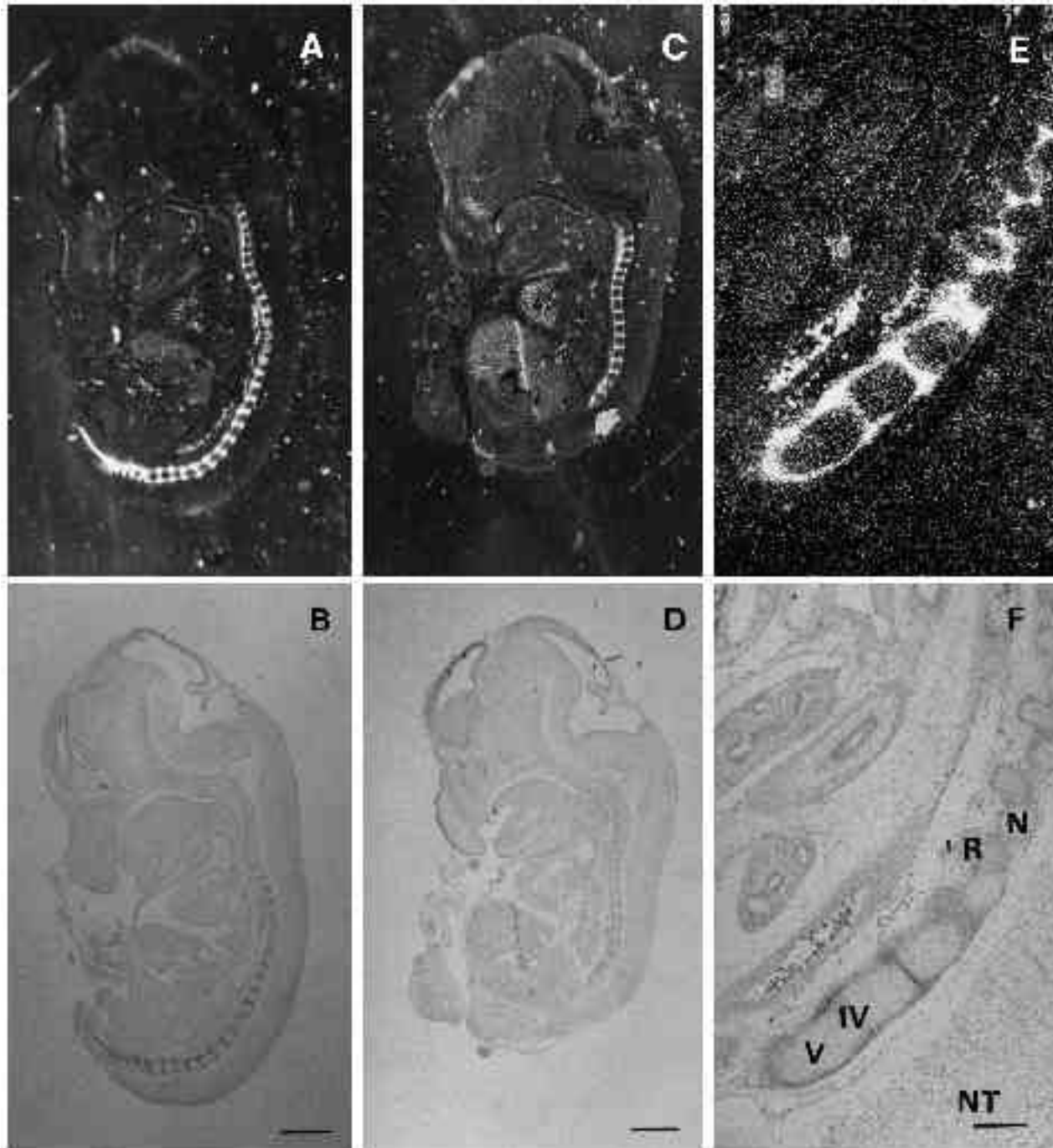


**Fig. 2.** *Pax-1* expression in wild-type and *Sd* homozygous embryos at day 13.5. (A) Parasagittal sections of wild-type embryos show more than 40 segmental *Pax-1* expression domains in the prospective vertebral column. Expression in the future sternum and the mesenchyme in the upper jaw can also be seen. (C) In *Sd* homozygotes, abrupt truncation of *Pax-1* expression domains in the developing vertebral column can be observed (indicated by an arrow). (E) Higher magnification view of the caudal end of the truncated axial skeleton of *Sd* homozygotes. Formation of vertebral bodies correlates with the number of *Pax-1* expression domains. Red blood cells in the aorta are giving background signals. (F) The structures are designated as follows, N, pedicles of neural arch anlagen; R, proximal parts of rib anlagen; IV, intervertebral disc anlagen; V, vertebral body anlagen, and NT, neural tube. B,D and F are bright-field views of the same section as shown in A,C and E, respectively. Scale bars, (B and D) 1 mm; (F) 250  $\mu$ m.

were always much more affected than the dorsal structures, for instance, the laminae of the neural arches (Fig. 1G).

The skeletal phenotype of the thoracolumbar region in *Sd* homozygotes revealed a significant similarity to that

produced by the different *un* alleles (Fig. 4A). From the 8th to the 10th thoracic vertebra (bold closed arrows in Fig. 4A), the ossification centers of each vertebral body were smaller or absent and occasionally bilaterally separated. These alter-

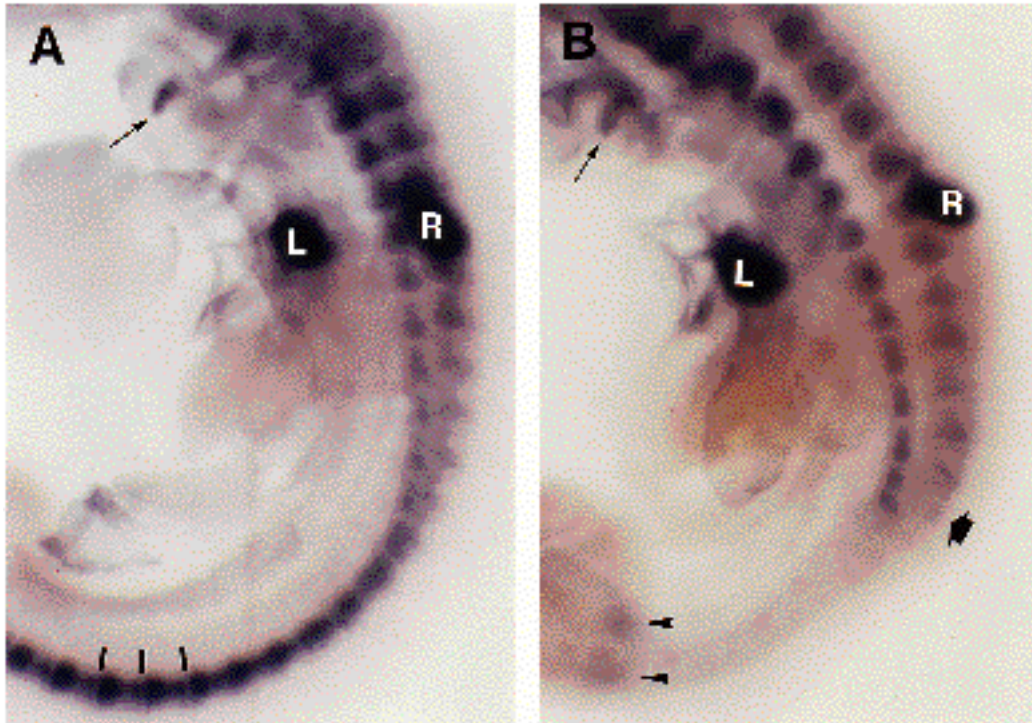


**Fig 3.** A comparison of *Pax-1* expression between wild-type (A) and *Sd* homozygous (B) embryos at day 10.5 by whole-mount in situ hybridization. *Pax-1* expression in the pharyngeal pouches are indicated by arrows. The expression of *Pax-1* in the left (L) and right (R) forelimb buds are also shown. In A, boundaries of several segmental units are indicated by bars. In B, the caudal end of the *Pax-1* expression domain in the paraxial mesoderm is indicated by the bold arrow. The expression of *Pax-1* in the hindlimb bud is indicated by arrowheads.

ations could also be observed in *Un<sup>s</sup>* heterozygotes (Fig. 1B). Between the 11th and 13th thoracic vertebrae the vertebral bodies were not formed and the pedicles of the neural arches protruded towards the midline and eventually fused (open arrows in Fig. 4A). Ribs often directly attach to the pedicle without forming a joint. This phenotype closely resembles abnormalities observed in *un<sup>ex</sup>* and *un* homozygotes (Fig. 4C; Wallin and Balling, unpublished data). In the lumbar region of the truncated vertebral column of *Sd* homozygotes, vertebral bodies and intervertebral discs were totally lost and only the neural arches were developed; this closely mimics the phenotype in *Un<sup>s</sup>* homozygotes (arrowheads in Fig. 4A).

*Un<sup>s</sup>* is the result of a complete deletion of the *Pax-1* locus with a semidominant genetic trait (Blandova and Egorov, 1975; Dietrich, Gruss and Balling, unpublished data). *undulated-extensive* (*un<sup>ex</sup>*) is a recessive mutation caused by the deletion of the last exon of the *Pax-1* gene, leading to a reduced amount of *Pax-1* transcripts (Wallace, 1985a; Dietrich, Gruss and Balling, unpublished data). The similarity of the phenotype produced by the *Sd* and *un* alleles suggests that the abnormalities of the vertebral column of *Sd* mutants might be the result of a reduction in the amount of *Pax-1* expression to a level similar to that found with the different *un* alleles.

#### Initial sclerotome formation does not require *Pax-1* expression

Differentiation of the somite into sclerotome and dermomyotome is known to correlate with changes in the expression of several genes. In wild-type embryos, the expression of *Pax-1* and *M-twist* colocalize in the sclerotome whereas *Pax-3* is exclusively expressed in the dermomyotome. *M-twist* codes for a protein with a helix-loop-helix domain,

which was isolated by sequence similarity to the *Drosophila twist* gene (Wolf et al., 1992). We used *M-twist* as an additional sclerotome marker. *Pax-3* is another member of the Pax gene family which is expressed in the epithelial somite and later in the dermomyotome (Goulding et al., 1991). To assess the sclerotome formation from the somite in the thoracolumbar region of *Sd* embryos, we analyzed the expression of *Pax-1*, *Pax-3* and *M-twist* at day 10.5 p.c. in adjacent sections. In *Sd* homozygotes, expression of *Pax-1* and *Pax-3* was compared using frontal sections. The expression of *Pax-1* in the paraxial mesoderm of the caudal part of *Sd*-embryos could not be observed at all while the expression in the cranial part was almost normal (Fig. 5A). *Pax-3* expression in adjacent sections localized only in the dermomyotome similar to what is seen in wild-type embryos (Fig. 5B; Goulding et al., 1991). The expression of *M-twist* in the sclerotome extended up to the 20th sclerotome while *Pax-1* expression had already stopped at the 18th sclerotome (Fig. 5D,E). This implies that the differentiation of the somites into the dermomyotome and the sclerotome has occurred in this region and suggests that deepithelialization of the somite is independent of the expression of *Pax-1*.

#### Structural changes of the notochord in *Sd* homozygotes

In order to analyze how and when the notochord of *Sd* homozygotes displays degenerative changes, the expression of the T (*Brachyury*) gene product was investigated, using a specific antiserum against a bacterially expressed fusion protein by whole-mount antibody staining (Kispert and Herrmann, 1993). As the first changes in *Pax-1* expression can be found at day 10.5, T-protein expression was investigated at day 9.5 and 10.5 (Fig. 6). Wild-type embryos at day 9.5 with 24 somites

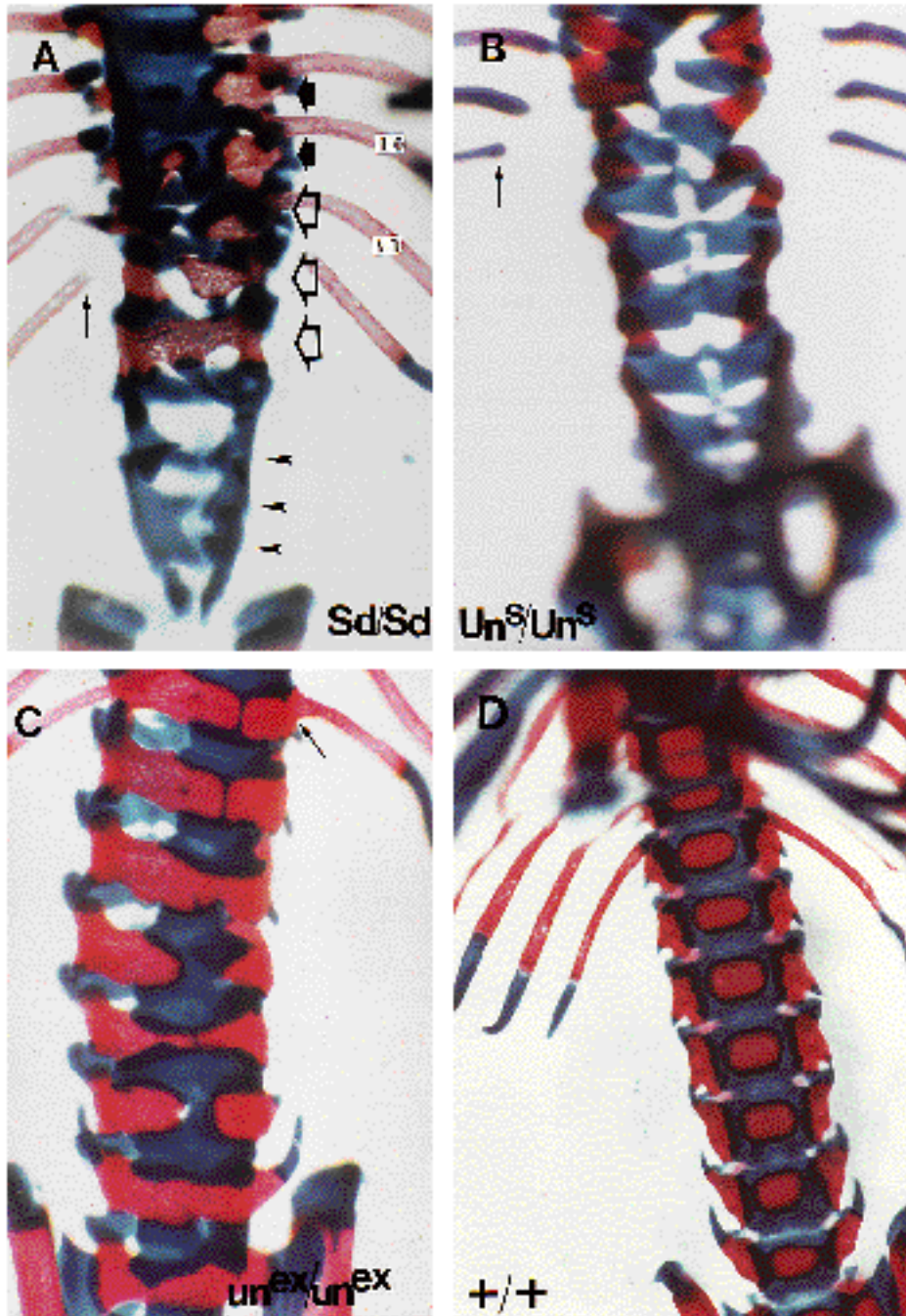


**Fig. 4.** A comparative analysis of the axial skeletal phenotype in the thoracolumbar region of *Sd/Sd* (A), *Un<sup>S</sup>/Un<sup>S</sup>* (B), *un<sup>ex</sup>/un<sup>ex</sup>* (C) and *+/+* (D) mice at the newborn stage. (A) *Sd* homozygotes. Note the cranio-caudal gradient in the severity of defects in the ventral structures of the vertebrae. Up to the 10th thoracic vertebra, vertebral bodies are formed although they have slight abnormalities such as split centra (closed bold arrows). From the 11th to 13th thoracic vertebrae, vertebral bodies and intervertebral discs are completely lost and pedicles of the neural arches are protruding towards the midline. The medioventrally protruding pedicles occasionally fuse (open bold arrows). Proximal parts of the ribs tend to float (thin arrow) or attach to the pedicle of the neural arch without proper joint formation (the proximal part of 11th left rib). In the lumbar region, vertebral bodies and intervertebral discs are completely lost and only neural arches are formed (arrowheads). In the more caudal part of *Sd* homozygotes, no cartilaginous or bony vertebral column can be seen. (B) *Un<sup>S</sup>* homozygote. None of vertebrae from the lower thoracic to the lumbar region have vertebral bodies or intervertebral discs whereas the formation of the neural arches is almost normal. The lower ribs are always floating (arrow). (C) *un<sup>ex</sup>/un<sup>ex</sup>* homozygote. Vertebral bodies and intervertebral discs are not formed in the ventral parts of the vertebrae but pedicles of neural arches are protruding towards the midline replacing the prospective vertebral bodies. Note that the proximal part of the rib attaches to the pedicle directly without joint formation (arrow). (D) Wild type mouse.

showed specific staining in the notochord from the infundibulum to the tailbud (Fig. 6A). The staining of the notochord was homogeneous and continuous. *Sd* homozygotes at the 21 somites stage also had notochord staining along the body axis including the tailbud (Fig. 6B). However, this staining was heterogeneous in the head and the cervical region and also discontinuous in the cervical region (Fig. 6B). Histological analysis revealed that T-protein-expressing cells are more dispersed in *Sd* homozygotes than in the wild type (data not shown). At day 10.5, wild-type embryos with 37 somites showed clear staining of the notochord and the tailbud as observed in day-9.5 embryos (Fig. 6C,E). *Sd* homozygotes with 35 somite pairs

showed considerable changes of the notochordal staining (Fig. 6D,F). In the cervicothoracic region, where the notochord was already stained at day 9.5, only rudimentary notochordal staining was occasionally seen (open arrow in Fig. 6D). In the caudal region, although the tailbud staining was similar to that found in wild-type embryos, expression of the T-protein in the notochord could not be observed at all. Not even a trace of the notochord seemed to be generated from the tailbud. The same observations were made in histological semithin sections (data not shown). Therefore the critical phase at which the notochord phenotype manifests itself in *Sd* embryos is between day 9.5 and 10.5 p.c.

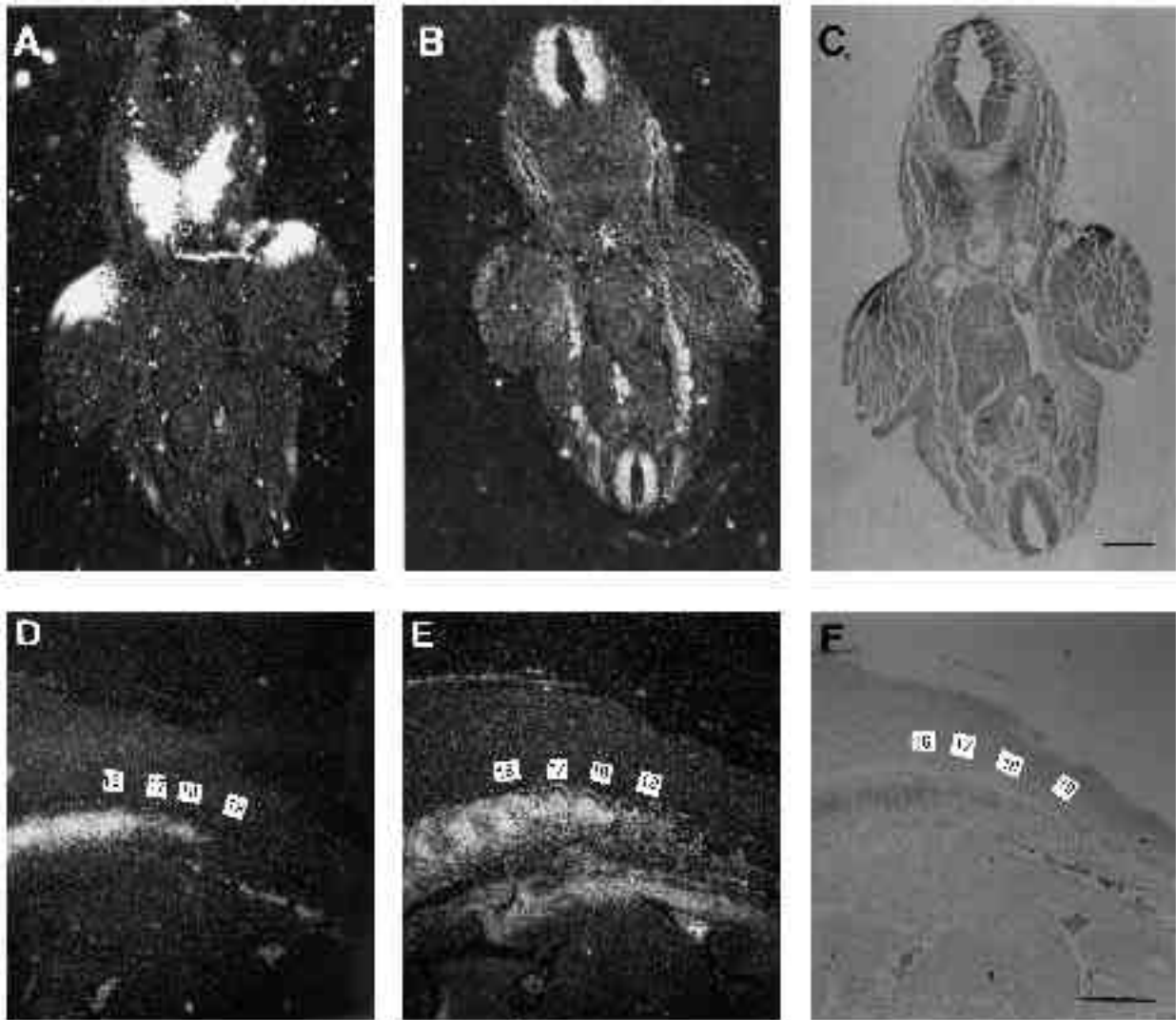


**Fig. 5.** A comparative analysis of the expression of *Pax-1*, *Pax-3* and *M-twist* in *Sd* homozygotes at day 10.5 using adjacent sections. (A) *Pax-1* expression in the paraxial mesoderm can only be observed in the cranial part but not in the caudal part as seen in Fig. 3B. The expression in the forelimb buds and lateral mesoderm is retained. (B) The expression of *Pax-3* in the adjacent section to that in A is shown. In the caudal part of the embryo, the *Pax-3* expression is localized in epithelial dermomyotomes while it is not observed in medial mesenchymal cells. Note that the expression of *Pax-3* in the neural tube is extending too much ventrally. (C) A bright-field view. Scale bar, 500  $\mu\text{m}$ . (D) *Pax-1* expression can be seen up to 18th sclerotome. The number of segmented structures in the paraxial mesoderm (sclerotome) starting from the proatlas is indicated by numbers in each figure. Note the significant reduction of *Pax-1* expression in the 17th and 18th sclerotomes and complete loss in the 19th and 20th sclerotomes. (E) *M-twist* expression can be observed in the paraxial mesoderm and mesonephros. The expression in the sclerotome apparently extends at least up to 20th segment. (F) A bright-field view. Scale bars, 300  $\mu\text{m}$ .

## DISCUSSION

In this study, we have begun a genetic and molecular dissection of the events leading to axial skeleton development by use of two mouse mutants, *Sd* and *un*. These mutants display primary abnormalities in the notochord and in the sclerotome, respectively (Grüneberg, 1954, 1958). The importance of the notochord for vertebral column development has been documented (Watterson et al., 1954; Grobstein and Holtzer, 1955). Recently Pourquie et al. (1993) have shown that a supernumerary notochord can induce additional vertebral bodies surrounding a trans-

planted notochord, but the molecular mechanisms of this process are poorly understood. We have analyzed the morphological changes of the notochord in *Sd* homozygous embryos using antibodies against the T protein, as a specific molecular marker. T is expressed in the entire notochord along the axis and in the tailbud at day-9.5 and -10.5 p.c. of normal mouse embryogenesis (Wilkinson et al., 1990; Kispert and Herrmann, unpublished data). Changes in the notochord in *Sd* homozygotes first appear between day 9.5 and 10.5. During this period, the notochord is affected in two different ways in *Sd* embryos. One is a degenerative change of the notochord (Paavola et al., 1980; Fig. 6). This

change manifests itself primarily in the prospective cervical and thoracic region. Another problem involves the tailbud from where the new notochord is generated. In *Sd* mutants, the tailbud apparently still has the ability to generate a notochord similar to wild-type embryos at day 9.5 p.c. However, this function of the tailbud is lost at day 10.5 p.c. (Grüneberg, 1958; Fig. 6E,F). This means that the notochord is never formed in the prospective lumbosacrocaudal region of *Sd* embryos. Nevertheless, formation of bilaterally segmented paraxial mesoderm from the tailbud can be seen at least up to day 11.5 p.c.

These observations imply that somites in the cranial part of *Sd* embryos, generated before day 9.5 of gestation, can differentiate in the presence of the notochord. However, somewhere between day 9.5 and 10.5 p.c. the mutant embryos lose the ability to generate a notochord so that more caudal somites are formed in the absence of any notochordal signals.

In the cranial part of the vertebral column, up to the 18th vertebra on average, the skeletal abnormalities are mild, showing decreased size of vertebral bodies. In this part of the body the somites have differentiated in the presence of a (degenerating) notochord. In the sacral-caudal region, cartilaginous structures are completely absent. The lack of a notochord in this region presumably results in a complete absence of sclerotome formation. In a transition zone between these two regions, comprising around five segments, we observed several vertebrae lacking ventral structures and being composed of neural arches only. Interestingly, this is the region where we can detect sclerotome formation but little or no *Pax-1* expression. It seems that in this particular region, where the notochord must have been present only transiently, we can separate the initial event of sclerotome formation and the induction, or maintenance, of *Pax-1* expression.

### Notochord signals induce *Pax-1* expression

The observed genetic interaction between *Sd* and both *un* (Wright, 1947; Grüneberg, 1953) and *Un<sup>s</sup>* (Fig. 1D) prompted us to analyze *Pax-1* expression in *Sd* mutant embryos. The results of that analysis support the notion that the notochord is required for normal *Pax-1* expression. First, a quantitative analysis of day-13.5 embryos revealed a significant reduction of *Pax-1* expression in *Sd* homozygotes and heterozygotes. Compound heterozygotes between *Sd* and *Un<sup>s</sup>* expressed less *Pax-1* than either of the single heterozygotes (data not shown). By in situ hybridization of day-10.5 embryos, *Pax-1* expression could be observed on average up to the 17th sclerotome in *Sd* homozygotes. In addition, in the last few segments we could detect a gradual loss of expression (Fig. 5D). We speculate that in the cervical-thoracic region, where we also have a clear interaction between the mutants, *Pax-1* expression might be slightly reduced but escaping detection for technical reasons. The notochord is more affected in the caudal part than in the cranial part. This indicates that *Pax-1* expression levels in sclerotome cells are tightly correlated with the changes of the notochord. These observations provide a molecular basis of the genetic interaction between *Sd* and *un*. In contrast to the *Pax-1* expression in the sclerotome, the expression in the hindlimb bud is apparently independent of the notochord.

In another mutant of the notochord, *T-curtailed* (*T<sup>c</sup>*; Searle, 1966), a similar correlation between notochord changes and *Pax-1* expression can be observed in the caudal region (data not shown). Furthermore, recent experiments in the chick support the stimulatory property of the notochord on *Pax-1* sclerotome expression. A supernumerary notochord transplanted in a dorsolateral position to the paraxial mesoderm, induces a widened *Pax-1* expression domain while suppressing dermomyotome differentiation (Brand-Sabieri et al., 1993). In summary, these data strongly support the idea that notochordal signals induce *Pax-1* expression. Whether this signal(s) is a diffusible molecule or is mediated via cell-cell or cell-matrix contacts is currently unknown.

### *Pax-1* expression is required for the formation of the ventral part of vertebrae but not for sclerotome induction

The skeletal phenotypes of *Sd* and the different *un* alleles display striking similarities. An analysis of *Un<sup>s</sup>*, *un<sup>ex</sup>* and *un* homozygotes demonstrates the requirement of *Pax-1* expression for proper formation of the ventral part of the vertebra in a dosage-dependent manner while the neural arches are apparently independent of the expression of *Pax-1* (Wallin and Balling, unpublished data). Observations on *Sd* homozygotes and compound heterozygotes between *Un<sup>s</sup>* and *Sd* reinforce this idea. The number of vertebral bodies seen in *Sd* homozygotes correlates well with the number of segmental *Pax-1* expression domains. Cumulative reduction of *Pax-1* expression by *Un<sup>s</sup>* and *Sd* mutations, predominantly affects the ventral part of vertebrae in the double heterozygous mutants.

The expression of *Pax-1* is normally tightly correlated with the formation of the sclerotome during differentiation of somites (Deutsch et al., 1988; Koseki and Balling, unpublished observations). Since the number of sclerotomes can be represented by that of the neural arches, sclerotome formation and *Pax-1* expression do not correlate strictly in *Sd* homozygotes. Sclerotomes are formed even if *Pax-1* is not expressed. A comparative analysis of *Pax-1*, *Pax-3* and *M-twist* also suggests that the process of sclerotome formation itself does not require *Pax-1*. Findings in *Un<sup>s</sup>* homozygotes further demonstrate this point. Normal sclerotome formation was observed in *Un<sup>s</sup>* homozygotes on day 10.5 p.c. embryos although *Pax-1* is completely deleted in this allele (Wallin and Balling, unpublished data).

In the present study, we provide evidence that formation of the vertebral column from the somites should be divided into two distinct processes as suggested previously (Cooper, 1965). The first is the formation of sclerotomes. This process depends on signals from the notochord and/or the ventral half of the neural tube, probably the floor plate (Watterson et al., 1954; Grobstein and Holtzer, 1955), but does not require *Pax-1*. A second process is the specification of sclerotome cells to obtain ventral or dorsal characteristics. We present evidence that without *Pax-1* expression sclerotome cells are unable to form ventral structures of the developing vertebrae. A striking similarity of the skeletal phenotype between embryos with *Sd* and *un* alleles suggests that *Pax-1* is one of the major responding elements of the notochordal signals within the sclerotome (Fig. 7).

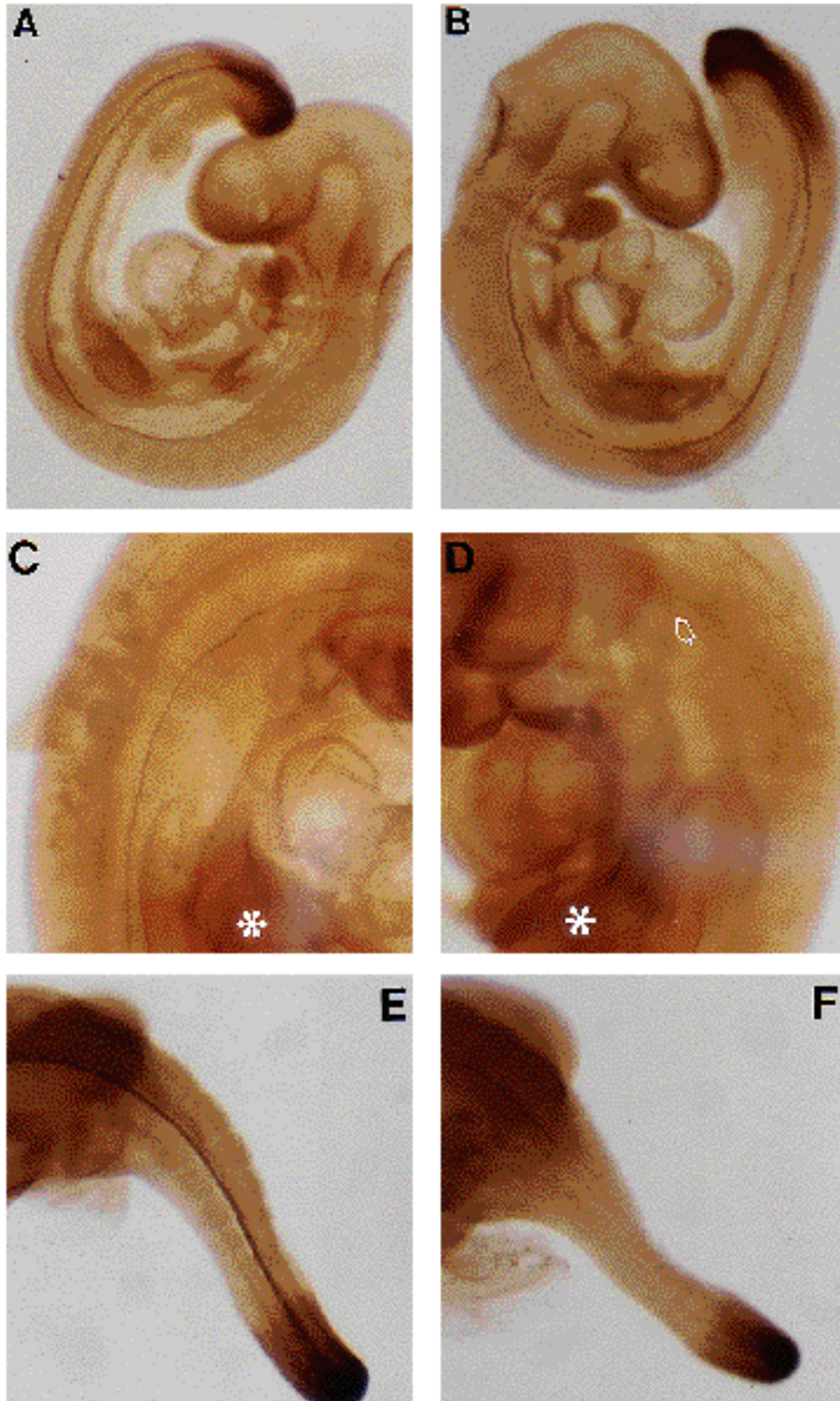


**Fig. 6.** The expression of T-protein in wild type and *Sd* mutant at day 9.5 and 10.5. (A) Wild-type embryo at day 9.5. (B) *Sd* homozygote at day 9.5. Note diffused and discontinuous notochord staining in *Sd* homozygotes. The cervicothoracic region of wild-type embryo at day 10.5 (C) and *Sd* homozygous embryo (D). In C and D, forelimb buds are indicated by asterisks. Rudimentary notochordal staining in the cervical region of *Sd* homozygote is pointed out by an open arrow. The caudal region of wild-type embryo (E) and *Sd* homozygote (F).

The formation of the dorsal part of vertebrae not only requires sclerotome formation but also a subsequent interaction between the dorsal half of the neural tube, including neural crest cells, and sclerotome cells (Watterson et al., 1954; Detwiler and Holtzer, 1956). This process seems to

be independent of *Pax-1*, but recent studies using the chick-quail chimera system indicate that cellular interactions between the surface ectoderm and the neural tube are important for the formation of the spinous process (Takahashi et al., 1992).

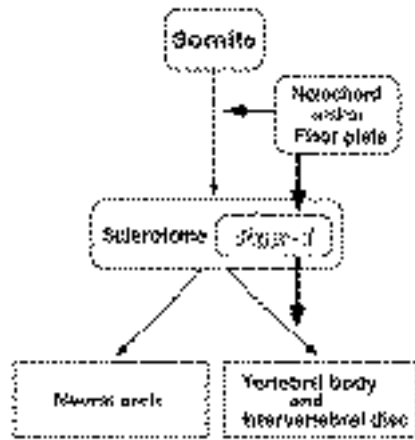


**Fig. 7.** The possible involvement of *Pax-1* in the differentiation of epithelial somites into the vertebral column. Cellular differentiation pathways are indicated by thin arrows while inductive cascades are shown by bold arrows. Signals from the notochord and/or the floor plate are necessary for the formation of the sclerotome from the epithelial somite and the induction of *Pax-1* expression in the sclerotome cells. *Pax-1* expression makes sclerotome cells competent to form the ventral parts of vertebrae. The formation of the neural arch does not require the expression of *Pax-1*.

### A role for Pax genes in dorsoventral patterning

Based on the present study, we suggest that both the notochord and *Pax-1* expression in sclerotome cells are necessary for formation of the ventral parts of vertebrae. At present the molecular mechanisms by which the notochord determines the dorsoventral (DV) polarity of the paraxial mesoderm and the neural tube are unknown. During mouse development, not only *Pax-1* but also at least eight other Pax genes are expressed with a distinct spatiotemporal pattern in the paraxial mesenchyme and/or the spinal cord (reviewed by Gruss and Walther, 1992; Wallin et al., 1993). Notochord transplantation and extirpation experiments in the chick have shown that *Pax-3* and *Pax-6* expression in the neural tube is dependent on the presence and precise spatial position of the notochord (Goulding et al., 1993). In the case of *Pax-3*, however, the notochord seems to have an inhibitory effect on *Pax-3* expression. In the prospective sacral region of *Sd* homozygotes, *Pax-3* expression becomes extended to the ventral half of the neural tube and of the paraxial mesoderm, as compared to normal embryos (Fig. 5B). Therefore, expression of *Pax-3* might be necessary for the specification of the neural cells localized in the dorsal half of the neural tube including the neural crest cells and for the specification of the dermomyotome. Since the mouse mutation *Splotch* (*Sp*) is a result of mutations in the *Pax-3* locus, an embryological analysis of *Sp* might be important to understand the role of *Pax-3* in the DV specification, not only in the neural tube, but also in the paraxial mesoderm (Epstein et al., 1991; Franz et al., 1993). A genetic interaction between *Sd* and *Sp* mutants might occur in a similar manner as seen for *un* and *Sd*. Interestingly, one of the modifiers of the *Sd* mutation maps close to the *Sp* locus (Wallace, 1985b).

In the lumbosacral region of *Sd* embryos the loss of the floor plate and the disorganization of motor axon guidance has been attributed to the loss of notochordal signals (Bovolenta and Dodd, 1991). For the specification of the floor plate, not only signals from the notochord (Yamada et al., 1991) but also the competence of the neural cells to respond to these signals are important. The formation of the floor plate is intrinsically affected in the zebrafish mutant, *cyclops*, where the floor plate is not formed although the signals from the notochord are intact (Hatta et al., 1991). The receptor for notochordal signals or downstream elements of this signal transduction pathway might be disturbed in this mutant, resulting in a loss of competence to form a floor plate. The role of notochordal signals and the competence of sclerotome cells for these signals might be comparable to the specification of the floor plate in the spinal cord. In this system, *Pax-1* would be required for interpretation of a notochordal signal in the process of the DV specification of the vertebral column. Therefore, similar mechanisms might exist for the DV specification of the neural tube and the vertebral column (Yamada et al., 1993).

We are grateful to Peter Gruss and Fabienne Perrin-Schmitt for the gift of the *Pax 1-8* and *M-twist* cDNA clones, respectively. We thank Michael Kessel, Wendy Pascoe, Klaus Schughart, Davor Solter, Claudio Stern and Steven Wood for comments on this manuscript and Johannes Schimers for technical assistance. H. K. was supported by an H. F. S. P. fellowship and J. W. was supported in part by an EMBO long-term fellowship and in part by the Swedish Medical Research Council. This work was made possible by financial support from the Max Planck Society and the DFG (Ba 869/3-1).

### REFERENCES

- Avery, G., Chow, M. and Holtzer, H. (1956). An experimental analysis of the development of the spinal column. V. Reactivity of chick somites. *J. Exp. Zool.* **132**, 409-425.
- Balling, R., Deutsch, U. and Gruss, P. (1988). *undulated*, a mutation affecting the development of the mouse skeleton, has a point mutation in the paired box of *Pax-1*. *Cell* **55**, 531-535.
- Balling, R., Lau, C. F., Dietrich, S., Wallin, J. and Gruss, P. (1991). Development of the skeletal system. *Ciba Found. Symp.* **165**, 132-143.
- Blandova, Z. R. and Egorov, I. U. (1975). *Sut* allelic with *un*. *Mouse News Lett.* **52**, 43.
- Bopp, D., Burri, M., Baumgartner, S., Frigerio, G. and Noll, M. (1986). Conservation of a large protein domain in the segmentation gene *Paired* and in functionally related genes of *Drosophila*. *Cell* **47**, 1033-1040.
- Bovolenta, P. and Dodd, J. (1991). Perturbation of neuronal differentiation and axon guidance in the spinal cord of mouse embryos lacking a floor plate: analysis of Danforth's short-tail mutation. *Development* **113**, 625-639.
- Brand-Saberi, B., Ebensperger, C., Wilting, J., Balling, R. and Christ, B. (1993). The ventralizing effect of the notochord on somite differentiation. *Anat. Embryol.* (in press).
- Center, E. M., Spigelman, S. S. and Wilson, D. B. (1982). Perichordal sheath of heterozygous and homozygous Danforth's short-tail mice. *J. Hered.* **73**, 299-300.
- Chalepakakis, G., Fritsch, R., Fickenscher, H., Deutsch, U., Goulding, M. and Gruss, P. (1991). The molecular basis of the *undulated/Pax-1* mutation. *Cell* **66**, 873-884.
- Christ, B. and Wilting, J. (1992). From somites to vertebral column. *Ann. Anat.* **174**, 23-32.
- Cooper, G. W. (1965). Induction of somite chondrogenesis by cartilage and notochord: A correlation between inductive activity and specific stages of cytodifferentiation. *Dev. Biol.* **12**, 185-212.

- Detwiler, S. R. and Holtzer, H. (1956). The developmental dependence of the vertebral column upon the spinal cord in the urodele. *J. Exp. Zool.* **132**, 299-310.
- Deutsch, U., Dressler, G.R. and Gruss, P. (1988). Pax-1, a member of a paired box homologous murine gene family, is expressed in segmented structures during development. *Cell* **53**, 617-625.
- Dietrich, W., Katz, H., Lincoln, S. E., Shin, H.-S., Friedman, J., Dracopoli, N. C. and Lander, E. S. (1992). A genetic map of the mouse suitable for typing intraspecific crosses. *Genetics* **131**, 423-447.
- Dunn, L. C., Gluecksohn-Schoenheimer, S. and Bryson, V. (1940). A new mutation in the mouse affecting spinal column and urogenital system. *J. Hered.* **31**, 343-348.
- Epstein, D. J., Vekemans, M. and Gros, P. (1991). *splotch* ( $Sp^{2H}$ ), a mutation affecting development of the mouse neural tube, shows a deletion within the paired homeodomain of *Pax-3*. *Cell* **67**, 767-774.
- Franz, T., Kothary, R., Surani, M. A. H., Halata, Z. and Grim, M. (1993). The *splotch* mutation interferes with muscle development in the limbs. *Anat. Embryol.* **187**, 153-160.
- Glisin, V., Crkvenjakov, R. and Byus, C. (1974). Ribonucleic acid isolated by cesium chloride centrifugation. *Biochemistry* **13**, 2633-2637.
- Gluecksohn-Schoenheimer, S. (1945). The embryonic development of mutants of the *Sd*-strain in mice. *Genetics* **30**, 29-38.
- Goulding, M. D., Chalepakis, G., Deutsch, U., Erselius, J. and Gruss, P. (1991). Pax-3, a novel murine DNA binding protein expressed during early neurogenesis. *EMBO J.* **10**, 1135-1147.
- Goulding, M. D., Lumsden, A. and Gruss, P. (1993). Signals from the notochord and floor plate regulate the region-specific expression of two Pax genes in the developing spinal cord. *Development* **117**, 1001-1016.
- Grobstein, C. and Holtzer, H. (1955). In vitro studies of cartilage induction in mouse somite mesoderm. *J. Exp. Zool.* **128**, 333-357.
- Grüneberg, H. (1953). Genetical studies on the skeleton of the mouse. VI. Danforth's short-tail. *J. Genet.* **51**, 317-326.
- Grüneberg, H. (1954). Genetical studies on the skeleton of the mouse. XII. The development of undulated. *J. Genet.* **52**, 441-455.
- Grüneberg, H. (1958). Genetical studies on the skeleton of the mouse. XXII. The development of Danforth's short-tail. *J. Embryol. exp. Morph.* **6**, 124-148.
- Gruss, P. and Walther, C. (1992). Pax in development. *Cell* **69**, 719-722.
- Hatta, K., Kimmel, C., Ho, R. and Walker, C. (1991). The cyclops mutation blocks specification of the floor plate of the zebrafish central nervous system. *Nature* **350**, 339-341.
- Kessel, M., Balling, R. and Gruss, P. (1990). Variations of cervical vertebrae after expression of a Hox-1.1 transgene in mice. *Cell* **61**, 301-308.
- Kessel, M. and Gruss, P. (1991). Homeotic transformations of murine vertebrae and concomitant alteration of Hox codes induced by retinoic acid. *Cell* **67**, 1-20.
- Kispert, A. and Herrmann, B. G. (1993). The Brachyury gene encodes a novel DNA binding protein. *EMBO J.* **12**, 3211-3220.
- Koseki, H., Jochen, Z., Mizutani, Y., Simon-Chazottes, D., Guenet, J.-L., Balling, R. and Gossler, A. (1993). Fine genetic mapping of the proximal part of mouse Chromosome 2 excludes *Pax-8* as a candidate gene for *Danforth's short tail* (*Sd*). *Mammalian Genome* **4**, 324-327.
- Jessell, T. M., Bovolenta, P., Placzek, M., Tessier-Lavigne, M. and Dodd, J. (1989). Polarity and patterning of the neural tube: the origin and function of the floor plate. *Ciba Found. Symp.* **144**, 255-280.
- Melton, D. A., Krieg, P. A., Rebagliati, M. R., Maniatis, T., Zinn, K. and Green, M. R. (1984). Efficient *in vitro* synthesis of biologically active RNA and RNA hybridization probes from plasmids containing a bacteriophage SP6 promoter. *Nucl. Acids Res.* **12**, 7035-7050.
- Paavola, L. G., Wilson, D. B. and Center, E. M. (1980). Histochemistry of the developing notochord, perichordal sheath and vertebrae in Danforth's short-tail (*Sd*) and normal C57BL/6 mice. *J. Embryol. exp. Morph.* **55**, 227-245.
- Placzek, M., Tessier-Lavigne, M., Yamada, T., Jessell, T. and Dodd, J. (1990). Mesodermal control of neural cell identity: floor plate induction by the notochord. *Science* **250**, 985-988.
- Pourquie, O., Coltey, M., Teillet, M.-A., Ordahl, C. and Le Douarin, N. M. (1993). Control of dorsoventral patterning of somitic derivatives by notochord and floor plate. *Proc. Natl. Acad. Sci. USA* **90**, 5242-5246.
- Rosen, B. and Beddington, R. S. P. (1993). Whole-mount in situ hybridization in the mouse embryo: gene expression in three dimensions. *Trends Genet.* **9**, 162-167.
- Searle, A.G. (1966). Curtailed, a new dominant T-allele in the house mouse. *Genet. Res., Camb.* **7**, 86-95.
- Takahashi, Y., Monsoro-Burq, A.-H., Bontoux, M. and Le Douarin, N. M. (1992). A role for *Quox-8* in the establishment of the dorsoventral pattern during vertebra development. *Proc. Natl. Acad. Sci. USA* **89**, 10237-10241.
- van Straaten, H. W. M. and Heckking, J. W. M. (1991). Development of floor plate, neurons and axonal outgrowth pattern in the early spinal cord of the notochord-deficient chick embryo. *Anat. Embryol.* **184**, 55-63.
- Wallace, M. E. (1985a). An inherited agent of mutation with chromosome damage in wild mice. *J. Hered.* **76**, 271-278.
- Wallace, M. E. (1985b). A modifier mapped in the mouse. *Genetica* **46**, 529.
- Wallin, J., Mizutani, Y., Imai, K., Miyashita, N., Moriwaki, K., Taniguchi, M., Koseki, H. and Balling, R. (1993). A new Pax gene, *Pax-9*, maps to mouse chromosome 12. *Mammalian Genome* **4**, 354-358.
- Wang, D., Villasante, A., Lewis, S. A. and Cowan, N. (1986). The mammalian  $\beta$ -tubulin repertoire: hematopoietic expression of a novel, heterologous  $\beta$ -tubulin isotype. *J. Cell Biol.* **103**, 1903-1910.
- Watterson, R. L., Fowler, I. and Fowler, B. J. (1954). The role of the neural tube and notochord in development of the axial skeleton of the chick. *Am. J. Anat.* **95**, 337-397.
- Wilkinson, D. G., Bhatt, S. and Herrmann, B. G. (1990). Expression pattern of the mouse T gene and its role in mesoderm formation. *Nature* **343**, 657-659.
- Wolf, C., Thisse, C., Stoetzel, C., Thisse, B., Gerlinger, P. and Perrin-Schmitt, F. (1992). The *M-twist* gene of *Mus* is expressed in subsets of mesodermal cells and is closely related to the *Xenopus X-twi* and *Drosophila twist* genes. *Dev. Biol.* **143**, 363-373.
- Wright, M. E. (1947). undulated: a new genetic factor in *Mus musculus* affecting the spine and tail. *Hered.* **1**, 137-141.
- Yamada, T., Placzek, M., Tanaka, H., Dodd, J. and Jessell, T. M. (1991). Control of cell pattern in the developing nervous system: polarizing activity of the floor plate and notochord. *Cell* **64**, 635-647.
- Yamada, T., Pfaff, S. L., Edlund, T. and Jessell, T. M. (1993). Control of cell pattern in the neural tube: motor neuron induction by diffusible factors from the notochord and floor plate. *Cell* **73**, 673-686.
- Youn, B. W. and Malacinski, G. M. (1980). Axial structure development in ultraviolet-irradiated (notochord-defective) amphibian embryos. *Dev. Biol.* **83**, 339-352.